Nanobioanalysis Hot Paper

Deutsche Ausgabe: DOI: 10.1002/ange.201503801
Internationale Ausgabe: DOI: 10.1002/anie.201503801

Real-time Monitoring of Discrete Synaptic Release Events and Excitatory Potentials within Self-reconstructed Neuromuscular Junctions**

Yu-Tao Li, Shu-Hui Zhang, Xue-Ying Wang, Xin-Wei Zhang, Alexander I. Oleinick, Irina Svir, Christian Amatore, and Wei-Hua Huang**

Abstract: *Chemical synaptic transmission is central to the brain functions. In this regard, real-time monitoring of chemical synaptic transmission during neuronal communication remains a great challenge. In this work, in vivo-like oriented neural networks between superior cervical ganglion (SCG) neurons and their effector smooth muscle cells (SMC) were assembled in a microfluidic device. This allowed amperometric detection of individual neurotransmitter release events inside functional SCG-SMC synapse with carbon fiber nanoelectrodes as well as recording of postsynaptic potential using glass nanopipette electrodes. The high vesicular release activities essentially involved complex events arising from flickering fusion pores as quantitatively established based on simulations. This work allowed for the first time monitoring in situ chemical synaptic transmission under conditions close to those found in vivo, which may yield important and new insights into the nature of neuronal communications.*

Chemical synaptic transmission is the process whereby one neuron communicates with other neurons or effector cells. As such this is crucial to the normal functioning of the nervous systems. Synapses are composed of presynaptic and postsynaptic membranes separated by a narrow (20–40 nm) cleft. In vivo, chemical synaptic transmission is elicited by an action potential arriving at the presynaptic button which provokes an influx of calcium ions through calcium-gated channels. This in turn causes the fusion of vesicles containing transmitters whose release and subsequent diffusion across the cleft lead to the activation of postsynaptic receptors giving rise to an action potential in the connected neuron or effector cell.[1] Great achievements in understanding vesicular transport, complex fusion machineries and mechanisms of vesicular neurotransmission have been made and were recognized by the 2000 Nobel Prize in Physiology or Medicine for signal transduction in the nervous system[2] and 2013 Nobel Prize in Physiology or Medicine for machinery regulating vesicle traffic.[3] However the very steps leading to release, that is, the synaptic vesicular exocytosis itself and its fast triggering of a postsynaptic signal are far from being fully understood.[4] Significant scientific challenges remain to be overcome to elucidate them based on their appropriate monitoring in vivo and in real time.

As the basic units of nerve system, mature neurons are elongated and highly branched to form synaptic connections with other neurons or target cells at extensions distant from the soma. Traditional Petri dish cultures do not allow enforcing spontaneous oriented axon growth to create synaptic connections similar to those forming in vivo where neuronal axons growth are guided by target neurons or effector cells. Conversely, microfluidic devices have recently offered powerful platforms for promoting spontaneous oriented elongation of axons from the soma, thus providing promising tools for in vitro spontaneous construction of functional neural networks.[5] On the other hand, amperometric electrochemical detection of chemical messengers release from single cells at ultramicroelectrodes has played a significant role in real-time monitoring of individual release events.[6] Great advances have been achieved in nanofabrication of nanometer-sized electrochemical sensors[7] prone to be used for amperometric measurements near or inside cells.[8] Recently, we were able to directly monitor single vesicular exocytotic events from inside single synapses with conical carbon fiber nanoelectrode (CFNE).[9] Measurement of action potentials stimulated by a receiving neuron after release by the exciting one would be ideally performed by patch clamp technique since this would offer both high signal-to-noise ratio and proper temporal resolution for postsynaptic membrane potential recording.[10] However, they are still important technical difficulties in patching subcellular structures such as neuron synaptic terminals.[11] Consequently, intracellular recording of electrical potential changes using nanopipettes potentiometric electrodes appears as the most effective mean to address this challenge.[12]

Herein, we take advantage of a novel and robust platform that incorporates the latest progresses in nanoprobes and

[*] Y. T. Li, S. H. Zhang, X. Y. Wang, X. W. Zhang, Prof. Dr. W. H. Huang
Key Laboratory of Analytical Chemistry for Biology and Medicine (Ministry of Education), College of Chemistry and Molecular Sciences, and LIA NanoBioCatEchem, Wuhan University
Wuhan 430072 (China)
E-mail: whhuang@whu.edu.cn
Dr. A. I. Oleinick, Prof. Dr. I. Svir, Prof. Dr. C. Amatore
Ecole Normale Supérieure, Département de Chimie, UMR 8640 (CNRS-ENS-UPMC and LIA NanoBioCatEchem
24 rue Lhomond, 75005 Paris(France)
E-mail: christian.amatore@ens.fr

[**] Supported by the National Natural Science Foundation of China (Nos. 21375099, 91017013), a Doctoral Fund of the Ministry of Education of China(20120141110031), the Fundamental Research Funds for the Central Universities (2042014kf0192), UMR 8640 (CNRS-ENS-UPMC), LIA NanoBioCatEchem, and ANR CHEX MicroNanoChem.

Supporting information for this article is available on the WWW under http://dx.doi.org/10.1002/anie.201503801.

microfluidics. However, in contrast with previous works involving such techniques[5] we use it to promote the spontaneous formation of synapses well-separated from the neuron bodies. This will serve for real-time monitoring of intrasynaptic release and subsequent generation of an electrical potential in a postsynaptic neuron terminal during synaptic chemical transmission in response to the K^+ stimulation of the distant neuron soma associated to the investigated synapse. Superior cervical ganglion (SCG) neurons and their effectors smooth muscle cells (SMCs) were cultured into two separate chambers of a microfluidic chip interconnected by a series of transverse microchannels. This allowed SCG axons guided-growth across the microchannels toward SMCs to spontaneously form intercellular communication SCG-SMC networks (Scheme 1 a).

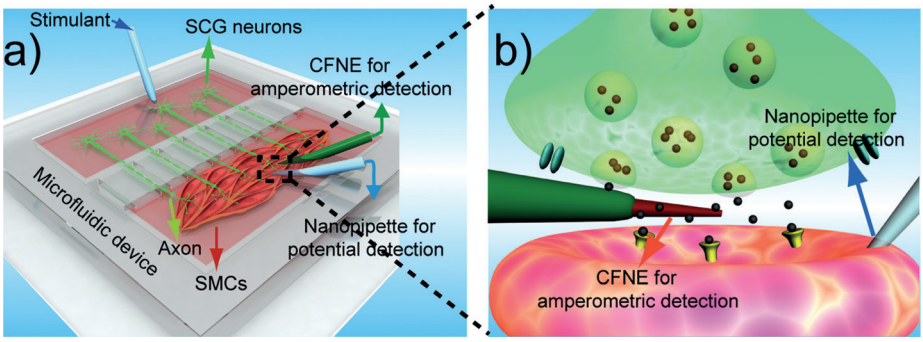

Scheme 1. a) Construction of in vivo-like neuromuscular junction (NMJ) in a microfluidic device. b) Representation of a carbon fiber nanoelectrode (CFNE) insertion inside a synapse for amperometric detection and of a glass nanopipette inside a smooth muscle cell (SMC) for post-synaptic potential recording.

This enabled us to insert a conical CFNE nanotip into functional SCG-SMC synapses for amperometric monitoring of single vesicular release events. Simultaneously, a glass nanopipette electrode was positioned inside the post-synaptic SMC cytoplasm for recording the postsynaptic potential responses triggered by the released neurotransmitters (Scheme 1 b). This work allowed the first in situ direct measurement of critical processes of chemical synaptic transmission under conditions close to those found in vivo.

Sympathetic innervation modulates the contractile activity of the vasculature and the growth of blood vessels through the neural interplay between SCG neurons and SMCs.[13] The spatially separated bodies of these cells are connected through elongated axons which form functional neuromuscular junctions (NMJ) with SMCs. Communication between SCGs and SMCs occurs at a distance from SCG soma through release of neurotransmitters inside NMJ synapses.[13b,c,d] Such precise targeted functional in vivo arrangements are almost impossible to systematically achieve with traditional Petri dish culture models (Supporting Information (SI), Figure S1). To overcome this difficulty we developed polydimethylsiloxane (PDMS) microfluidic chips in which SCG neurons and SMCs were separately cultured in parallel compartments connected through a net of microgrooves (5 μm wide, 2.5 μm high; Figure 1 a,b; see more in the Supporting Information) microfabricated by standard soft lithography techniques. Dissociated SCG neurons and SMCs were seeded into each respective compartment and cultured for a certain amount of time (ca. 3–4 days). SCG axons extended into the microgrooves up to the SMC compartment where they formed NMJ with SMCs (Figure 1 a–c, Supplementary Movie 1 and Movie 2). Directional axons growth and NMJ formation were efficiently promoted by the effector cells (data not shown). Immunocytochemistry clearly demonstrated the physical isolation of axons (stained for tyrosine hydroxylase (TH), green) from somata via the axon-guiding microgrooves to formed NMJ with SMCs (stained for α-actin, red) (Figure 1 b,c).

In vivo, acetylcholine (ACh) released from preganglionic sympathetic nerve terminals stimulates norepinephrine (NE) release from postganglionic nerve terminals that then act on SMCs,[14] and intracellular calcium concentration shows increase in both postganglionic nerve terminals and SMCs during this process.[14,15] The neural networks grown in the microfluidic chips displayed an identical behavior. Intracellular calcium levels were detected by preloading Fluro4-AM into cells. The percentages of fluorescence intensity increase ($(F-F_0)/F_0$, $\Delta F/F_0$, Figure 1 d) allowed assessing to which extent functional junctions had been formed between SCG neurons and SMCs. When SMC

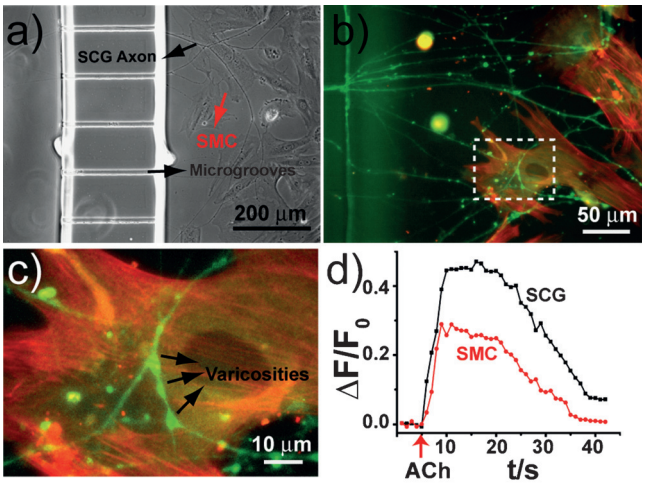

Figure 1. a,b) Bright-field (a) and fluorescent (b) microphotographs showing the isolation and oriented elongation of axons from the soma via interconnecting microgrooves to form in vivo-like neuromuscular junction (NMJ); SCG neurons were labeled with tyrosine hydroxylase primary antibody (green), SMCs were labeled with α-actin primary antibody (red). c) Amplified picture of dotted frame in (b) showing 3 varicosities tightly attached on SMC. d) Acetylcholine (ACh) stimulates increases in cytosolic free calcium concentration inside both SCG neuron (black line) and SMC (red line) in SCG/SMC co-culture system.

were cultured alone in the absence of SCG neurons, 10^{-4} M NE elicited an increase ($\Delta F/F_0 = 0.52 \pm 0.03$, mean $\pm$ SE) in intracellular calcium concentration while the addition of ACh (10^{-4} M) did not induce any increase in intracellular calcium concentration (data not shown) evidencing that SMC were functional and confirming that ACh alone could not directly regulate intracellular calcium level in SMC. Conversely, in SCG and SMC co-cultured system, stimulation by ACh caused an increase in intracellular calcium concentration in both SCG neurons (Figure 1 d, black line, $\Delta F/F_0 = 0.45 \pm 0.02$, $n = 3$) and SMCs (Figure 1 d, red line, $\Delta F/F_0 = 0.28 \pm 0.01$, $n = 3$), indicating that ACh can indirectly modulate intracellular calcium level in SMC through activation of SCG neurons as occurs in vivo. Beyond morphological microscopic observations this established that functional junctions spontaneously formed between postganglionic sympathetic neurons and SMC in the co-culture microchips.

Conical carbon fiber nanoelectrodes (CFNEs) were prepared as previously reported.[9] Briefly, a glass sub-micropipette pulled by a laser micropuller was used to seal and insulate flame-etched[16] carbon nanofiber; the protruding conical nanotip was further etched with a microforge to provide a very fine electroactive tip of 50–200 nm diameter with a controlled 500–2000 nm shaft length (Figure 2 a, Figure S2). After formation of functional NMJ with SMCs, a CFNE nanotip was slipped into a randomly selected SCG-SMC synapse located in the SMC compartment for amperometric detection (Scheme 1 a, Figure 2 b). The interest of using the microfluidic platform described above was that the selected synapse could be tracked back through microscopy to SCG neuron soma in the SCG compartment. This allowed to specifically stimulate it with a 70 mM K^+ pulse while ensuring that no unwanted stimulation occurred near the investigated synapse, thus mimicking actual neuronal behavior (note that this contrast with the measurements we reported previously).[9] This elicited a series of well-defined amperometric spikes after a short time delay ($T_{tr} \approx 1$–5 s, Figure 2 c). A high percentage of events displayed in the amperometric trace exhibited a complex structure (59.8 %, 137 complex spikes from 229 events) similar to those previously recorded in conventional Petri dish co-culture system and ascribed to flickering fusion pores.[9] Complex events comprised a series of short related spikes emitted over longer overall durations ($t_{1/2} = 1.27 \pm 0.09$ ms, mean $\pm$ s.e.m., Figure 2 c) which differed from the single-spike features of simple events ($t_{1/2} = 0.43 \pm 0.01$ ms, Figure 2 d). Furthermore, compared with the single-Gaussian distribution of amperometric peak height of simple events, complex events revealed a bimodal distribution with a larger population centered at ca. 5 pA and a smaller one centered at ca. 9 pA, that is, approximately equal to that of simple events (Figure 2 e). Precise simulations[17] of flickering current intensities displayed during complex events established that these events corresponded to fusion pores transiently opening up to a radius of ca. 1.2 nm and closing again (Figure 3). Interestingly, as from patch-clamp measurements on endocrine catecholaminergic cells, 1.2 nm is the mean radius value of initial fusion pores.[18] Since the machineries giving rise to initial pore formation (SNAREs, etc.)[4c] are expected to be involved in catecholaminergic neurons, this result strongly suggest that complex events correspond to rapid flickering of initial fusion pores (Kiss and Run)[10] although they lead to almost full release. Indeed the average number of released molecules (53 000 in Figure 3, yet 33 000 for all complex events) matches the expected number for this type of vesicles.[20]

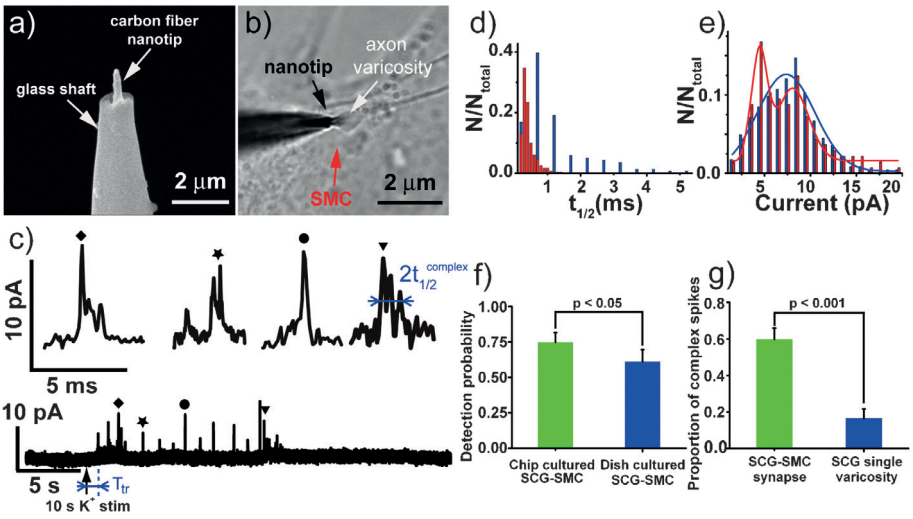

Figure 2. Nanoelectrode amperometric monitoring of vesicular release of neurotransmitters inside synapses formed between SCG neurons and SMC inside microfluidic chip. a) SEM of a carbon fiber nanoelectrode. b) Bright-field photomicrographs showing the tip of a sensor inserted inside a synapse between a varicosity of a SCG neuron and a SMC. c) High K^+-induced amperometric spikes with the four labeled typical complex events being enlarged above (enlarged views of simple events are not shown since they display a single spike). d,e) Histograms of simple (red) versus complex (blue) events $t_{1/2}$ characteristics ($n = 219$ for simple events and $n = 240$ for complex ones; see $t_{1/2}$ definition in (c) or maximum current peak intensities ($n = 294$ for simple events and $n = 401$ for complex ones). f) Detection probabilities inside SCG-SMC synapses forming spontaneously in chips versus those formed statistically in Petri dish co-cultures. g) Detection probabilities of complex spikes ($n = 92$) detected inside SCG-SMC synapses in chip-cultured systems versus above single varicosities; error bars represent standard errors, and independent-samples T test was used to calculate P values.

The present results and those we reported from measurements in conventional Petri dishes co-cultures show phenomenological agreement but led to significantly different detection probabilities (Figure 2 f). The detection probability inside NMJ synaptic clefts spontaneously constructing in chips was 74.6 %, being higher ($p < 0.05$) than that for Petri dish cultured ones (61.0 %). This suggests that NMJ junctions spontaneously formed by SCG axons guided by

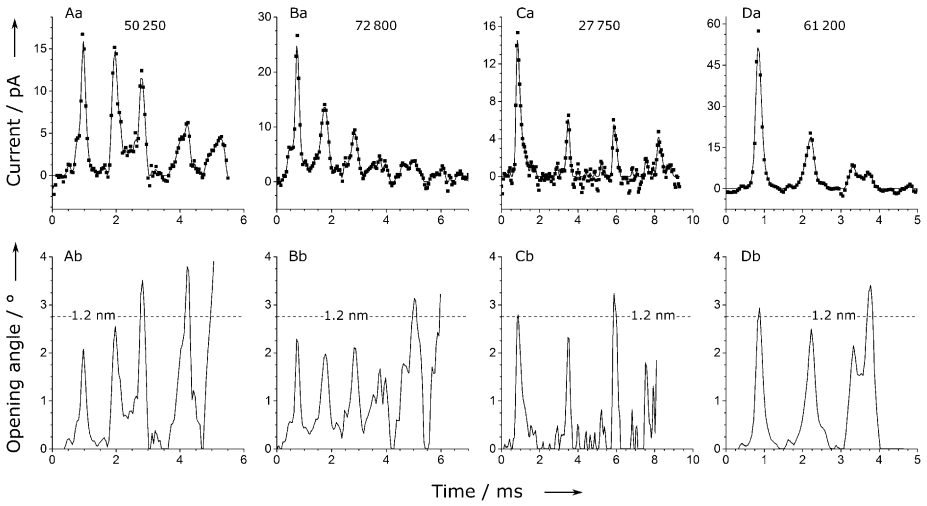

Figure 3. Top row: Physico-mathematical simulations of the current intensities of four different typical complex events (data points indicate actual current measurements and solid curves the reconstructed currents; the overall number of molecules released during each complex event is indicated in each panel). Bottom row: Time variations of fusion pores angular aperture (in degrees) reconstructed from the simulations for each complex event shown immediately above (the horizontal line is the limit expected for a fusion pore radius of 1.2 nm assuming a mean vesicle radius of 25 nm).[4c,19] Simulations were performed assuming a diffusion rate of 4.0×10^4 s^{-1} of catecholamine cations inside vesicles during release. No other adjustable parameter was used. (See SI and Ref. [17]).

their effector cells resembled more closely to in-vivo neural connections than those formed statistically in conventional Petri dish co-cultures of both cell types (Figure S1).

Remarkably, large differences were observed in the complex events percentages between measurements inside NMJ clefts (59.8%) and on isolated varicosities that did not formed NMJ synapses (16.6%). High percentage of complex events occurred inside functional synapses, being much larger than for isolated varicosities ($p < 0.001$, Figure 2g), again suggesting that the present methodology led to the formation neural chains closely mimicking real ones. Indeed, the results in Figure 3 evidence that these complex events featured Kiss and Run release rather than Extended Kiss and Run[21] or Full Fusion that would correspond to much larger fusion pore radii.

To examine the innervation of SCG neuron on SMCs, postsynaptic membrane potentials were recorded using conventional glass microelectrodes rather than by patch clamp since cultured SMC could not yield high resistance seals required by the latter. Intracellular recording of membrane potential were thus monitored by inserting a glass nanopipette electrode (GNPE) inside the target SMC cytoplasm. GNPEs were fabricated from borosilicate capillaries with filaments using a Sutter P-2000 laser puller (see supporting information); the inner diameters of the resulting tips were controlled to be less than 300 nm (Figure 4a,b).

The ability of GNPEs inserted in SMCs for measuring cell membrane potential changes during long-time recordings was first assessed. Measurements were carried out with a high impedance amplifier at zero current. Figure 4d shows the electrical potential changes during a typical electrophysiological experiment involving a KCl filled GNPE penetration inside a cell and its subsequent withdrawal. The potential dropped steeply when a nanopipette crossed the cell membrane and gradually settled at a constant level while the cell membrane sealed around its shaft forming a high-resistance seal with the GNPE[12a] thus allowing measuring the stable rest transmembrane potential (RMP) at ca. 42 mV. After the GNPE was withdrawn from the cell the potential returned to its extracellular zero value. GNPEs were then tested for intracellular monitoring of spontaneous activity of SCG neurons. Inserting a GNPE into an SCG soma allowed recording an action potential typical for SCG neurons (about 40 mV, inset of Figure 4d). This series of tests successfully validated the principle of transmembrane potential measurement with GNPEs.

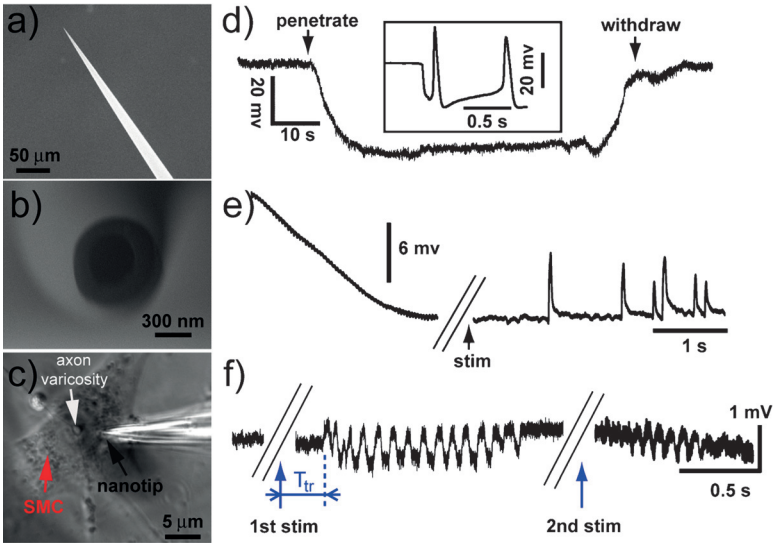

Figure 4. Measurement of cell membrane potentials with glass nanopipettes (GNPEs). a,b) Scanning electron microscopic pictures showing the global (a) and amplified view (b) of a GNPE. c) Bright-field photomicrographs showing the tip of a nanopipette inside a SMC forming a functional NMJ with the SCG varicosity closely attached to it. d) Changes in electrical potential during a typical electrophysiology experiment during penetration and withdrawal of a GNPE from the SMCs (arrows); inset is a typical action potential trace recorded upon inserting a GNPE into a SCG soma. e) Representative trace of a SMC membrane potential triggered by a 10^{-6} M NA puff onto it. f) Trace of a postsynaptic SMC membrane potential after puffing 70 mM K^+ to stimulate SCG neuron.

GNPEs were then used to electrically record postsynaptic cell responses (excitatory junction potential, EJP) following presynaptic neurons stimuli. After the penetration of GNPE into the SMC and formation a high-resistance seal (Figure 4c), control experiments showed that 10^{-6} M NE stimulating pulses successfully elicited a sequence of EJP signals (5–10 mV, $n = 10$) in chips co-cultured SMCs (Figure 4e). This indicated that physiological NE-stimulation of the whole SMC terminal region produced EJPs as those recorded in vivo, i.e., that the post-synaptic/SMC terminals domains formed under our conditions exposed an adequate amount of functional NE-receptors. However, there are reported indications that the number of receptors present within freshly formed synaptic clefts, as investigated here, may be less than occurs in vivo in trained synapses since a non-negligible fraction of receptors may still have to diffuse across the postsynaptic membranes to settle inside the synaptic cleft.[22]

To test for this issue, local micro-puffs of 70 mM K^+ were applied in the SCG compartment onto the soma or the axon of the presynaptic neuron specifically connected to the investigated SMC. Since it was shown above that under our conditions release events preferentially occurred inside synaptic clefts (Figure 2g) without significant activity of varicosities this procedure allowed scrutinizing the reception efficiency inside the freshly constructed synapses. Compared with the signal triggered by local external stimulation of SMC by NE, the ensuing EJP signals elicited 1–5 s time after the K^+ stimulation by NE released inside synaptic clefts yielded quite small membrane potential signals (0.5–1.5 mV). These consisted in characteristic trains of oscillatory membrane potential pursued over half a second to a few seconds (Figure 4f) being reproducible and perfectly identifiable physiologically. The magnitude and frequency of intrasynaptic release events (Figure 2) detected by CFNE measurements suggest that a decrease of efficiency in intrasynaptic NE release could not be invoked to account for such reduced EJP signals albeit low NE doses are known to yield very small potential changes down to 1 mV.[23] Hence, though other unknown factors may play a role it is likely that the reduced EJP signals in Figure 4f are consistent with a too feeble number of receptors being yet present into the intrasynaptic sections of the SMC membranes in our freshly formed synapses.[22]

In summary, in vivo-like oriented neural networks and functional NMJ could be reconstructed in microfluidic chips, allowing monitor individual vesicular release events inside synapses as well as the evoked postsynaptic potential signals in real time by using two kinds of nanoelectrochemical sensors. The present results established that axon terminals guided by their effector cells across relatively long distances compared to their soma form functional junctions and display high vesicular release activities. Complex vesicular exocytosis involving flickering pores formation appears as the major mode of fusion for NE release from inside these reconstructed SCG-SMC synapses. Furthermore, vesicularly NE release following K^+ stimulation of the distant presynaptic specific SCG neuron could effectively trigger postsynaptic membrane potential signals in SMCs. Though the EJP signals resulted smaller than those occurring in vivo in trained junctions, their successful recording evidenced the adequate functionality of SCG-SMC spontaneously reconstructing in the microchips. Albeit the reason for smaller action potentials remains to be better understood, this work allow the first in situ direct measurement of critical integrated processes in chemical synaptic transmission under conditions close to in vivo situations.

Keywords: microfluidic chip · nano-sensors · neuronal communication · synapse

How to cite: *Angew. Chem. Int. Ed.* **2015**, *54*, 9313–9318
Angew. Chem. **2015**, *127*, 9445–9450

[1] a) T. M. Jessell, E. R. Kandel, *Cell* **1993**, *72*, 1–30; b) E. R. Kandel, J. H. Schwartz, T. M. Jessell, *Principles of Neural Science*, 4th ed., McGraw-Hill, New York, **2000**; c) V. Di Maio, *Brain Res.* **2008**, *1225*, 26–38; d) C. Ribrault, K. Sekimoto, A. Triller, *Nat. Rev. Neurosci.* **2011**, *12*, 375–687.

[2] *Signal transduction in the nervous system* in The Nobel Prize in Physiology or Medicine 2000 press release, Oct. 9, **2000**.

[3] *Machinery regulating vesicle traffic, a major transport system in our cells* in The Nobel Prize in Physiology or Medicine press release 2013, Oct. 7, **2013**.

[4] a) V. Haucke, E. Neher, S. J. Sigrist, *Nat. Rev. Neurosci.* **2011**, *12*, 127–138; b) P. M. Casillas-Espinosa, K. L. Powell, T. J. O'Brien, *Epilepsia* **2012**, *53*, 41–58; c) A. A. Alabi, R. W. Tsien, *Annu. Rev. Physiol.* **2013**, *75*, 393–422; d) T. C. Südhof, *Neuron* **2013**, *80*, 675–690.

[5] a) R. B. Campenot, *Proc. Natl. Acad. Sci. USA* **1977**, *74*, 4516–4519; b) A. M. Taylor, M. Blurton-Jones, S. W. Rhee, D. H. Cribbs, C. W. Cotman, N. L. Jeon, *Nat. Methods* **2005**, *2*, 599–605; c) J. El-Ali, P. K. Sorger, K. F. Jensen, *Nature* **2006**, *442*, 403–411; d) M. S. Cohen, C. B. Ortha, H. J. Kimb, N. L. Jeonc, S. R. Jaffrey, *Proc. Natl. Acad. Sci. USA* **2011**, *108*, 11246–11251; e) L. J. Millet, M. U. Gillette, *Trends Neurosci.* **2012**, *35*, 752–761; f) C. A. Croushore, J. V. Sweedler, *Lab Chip* **2013**, *13*, 1666–1676; g) N. Lee, J. W. Park, H. J. Kim, J. H. Yeon, J. Kwon, J. J. Ko, S. H. Oh, H. S. Kim, A. Kim, B. S. Han, S. C. Lee, N. L. Jeon, J. Song, *Mol. Cells* **2014**, *37*, 497–502.

[6] a) R. M. Wightman, J. A. Jankowski, R. T. Kennedy, K. T. Kawagoe, T. J. Schroeder, D. J. Leszczyszyn, J. A. Near, Jr., E. J. Diliberto, O. H. Viveros, *Proc. Natl. Acad. Sci. USA* **1991**, *88*, 10754–10758; b) E. V. Mosharov, D. Sulzer, *Nat. Methods* **2005**, *2*, 651–658; c) A. Schulte, W. Schuhmann, *Angew. Chem. Int. Ed.* **2007**, *46*, 8760–8777; *Angew. Chem.* **2007**, *119*, 8914–8933; d) C. Amatore, S. Arbault, M. Guille, F. Lemaitre, *Chem. Rev.* **2008**, *108*, 2585–2621; e) Y. X. Huang, D. Cai, P. Chen, *Anal. Chem.* **2011**, *83*, 4393–4406.

[7] a) R. W. Murray, *Chem. Rev.* **2008**, *108*, 2688–2720; b) J. T. Cox, B. Zhang, *Annu. Rev. Anal. Chem.* **2012**, *5*, 253–272; c) Y. Takahashi, A. I. Shevchuk, P. Novak, Y. Zhang, N. Ebejer, J. V. Macpherson, P. R. Unwin, A. J. Pollard, D. Roy, C. A. Clifford, H. Shiku, T. Matsue, D. Klenerman, Y. E. Korchev, *Angew. Chem. Int. Ed.* **2011**, *50*, 9638–9642; *Angew. Chem.* **2011**, *123*, 9812–9816; d) B. Zhang, L. Fan, H. Zhong, Y. Liu, S. Chen, *J. Am. Chem. Soc.* **2013**, *135*, 10073–10080; e) X. Zhu, Y. Qiao, X. Zhang, S. Zhang, X. Yin, J. Gu, Y. Chen, Zhu, Z. M. Li, Y. Shao, *Anal. Chem.* **2014**, *86*, 7001–7008.

[8] a) W. Z. Wu, W. H. Huang, W. Wang, Z. L. Wang, J. K. Cheng, T. Xu, R. Y. Zhang, Y. Chen, J. Liu, *J. Am. Chem. Soc.* **2005**, *127*, 8914–8915; b) P. Sun, F. O. Laforge, T. P. Abeyweera, S. A. Rotenberg, J. Carpino, M. V. Mirkin, *Proc. Natl. Acad. Sci. USA* **2008**, *105*, 443–448; c) X. T. Zheng, C. M. Li, *Chem. Soc. Rev.* **2012**, *41*, 2061–2071; d) Y. Wang, J. M. Noel, J. Velmurugan, W. Nogala, M. V. Mirkin, C. Lu, M. G. Collignon, F. Lemaitre, C. Amatore, *Proc. Natl. Acad. Sci. USA* **2012**, *109*, 11534–11539;

e) P. Actis, S. Tokar, J. Clausmeyer, B. Babakinejad, S. Mikhaleva, R. Cornut, Y. Takahashi, A. López Córdoba, P. Novak, A. I. Shevchuck, J. A. Dougan, S. G. Kazarian, P. V. Gorelkin, A. S. Erofeev, I. V. Yaminsky, P. R. Unwin, W. Schuhmann, D. Klenerman, D. A. Rusakov, E. V. Sviderskaya, Y. E. Korchev, *ACS Nano* **2014**, *8*, 875 – 884.

[9] Y. T. Li, S. H. Zhang, L. Wang, R. R. Xiao, W. Liu, X. W. Zhang, Z. Zhou, C. Amatore, W. H. Huang, *Angew. Chem. Int. Ed.* **2014**, *53*, 12456 – 12460; *Angew. Chem.* **2014**, *126*, 12664 – 12668.

[10] a) E. Neher, B. Sakmann, *Nature* **1976**, *260*, 799 – 802; b) B. Sakmann, E. Neher, *Annu. Rev. Physiol.* **1984**, *46*, 455 – 472; c) A. M. Gurney, *J. Pharmacol. Toxicol. Methods* **2000**, *44*, 409 – 420; d) A. Verkhratsky, O. A. Krishtal, O. H. Petersen, *Pflugers Arch.* **2006**, *453*, 233 – 247.

[11] a) Y. Zhao, S. Inayat, D. A. Dikin, J. H. Singer, R. S. Ruoff, J. B. Troy, *Proc. Inst. Mech. Eng. Part N* **2008**, *222*, 1 – 11; b) M. E. Spira, A. Hai, *Nat. Nanotechnol.* **2013**, *8*, 83 – 94.

[12] a) M. G. Schrlau, N. J. Dun, H. H. Bau, *ACS Nano* **2009**, *3*, 563 – 568; b) X. Duan, R. Gao, P. Xie, T. Cohen-Karni, Q. Qing, H. S. Choe, B. Tian, X. Jiang, C. M. Lieber, *Nat. Nanotechnol.* **2012**, *7*, 174 – 179; c) J. T. Robinson, M. Jorgolli, A. K. Shalek, M. H. Yoon, R. S. Gertner, H. Park, *Nat. Nanotechnol.* **2012**, *7*, 180 – 184; d) C. Xie, Z. Lin, L. Hanson, Y. Cui, B. Cui, *Nat. Nanotechnol.* **2012**, *7*, 185 – 190; e) Z. C. Lin, C. Xie, Y. Osakada, Y. Cui, B. Cui, *Nat. Commun.* **2014**, *5*, 1 – 10.

[13] a) S. E. Luff, *Anat. Embryol.* **1996**, *193*, 515 – 531; b) M. R. Bennett, A. Cheung, K. L. Brain, *Microsc. Res. Tech.* **1998**, *42*, 433 – 450; c) M. R. Bennett, *News. Physiol. Sci.* **1998**, *13*, 79 – 84; d) G. Burnstock, *Annu. Rev. Pharmacol. Toxicol.* **2009**, *49*, 1 – 30.

[14] D. H. Damon, *Am. J. Physiol-Heart C* **2000**, *278*, H404 – H411.

[15] D. Atlas, *Annu. Rev. Biochem.* **2013**, *82*, 607 – 635.

[16] a) T. G. Strein, A. G. Ewing, *Anal. Chem.* **1992**, *64*, 1368 – 1373; b) W. H. Huang, D. W. Pang, H. Tong, Z. L. Wang, J. K. Cheng, *Anal. Chem.* **2001**, *73*, 1048 – 1052.

[17] a) C. Amatore, A. I. Oleinick, I. Svir, *ChemPhysChem* **2010**, *11*, 149 – 158; b) C. Amatore, A. I. Oleinick, I. Svir, *ChemPhysChem* **2010**, *11*, 159 – 174; c) A. Oleinick, F. Lemaître, M. Guille Collignon, I. Svir, C. Amatore, *Faraday Discuss.* **2013**, *164*, 33 – 55.

[18] A. Albillos, G. Dernick, H. Horstmann, W. Almers, G. A. deToledo, M. Lindau, *Nature* **1997**, *389*, 509 – 512.

[19] L. He, X. S. Wu, R. Mohan, L. G. Wu, *Nature* **2006**, *444*, 102 – 105.

[20] Z. Zhou, S. Misler, *Proc. Natl. Acad. Sci. USA* **1995**, *92*, 6938 – 6942.

[21] a) R. G. W. Staal, E. V. Mosharov, D. Sulzer, *Nat. Neurosci.* **2004**, *7*, 341 – 346; b) R. M. Wightman, C. L. Haynes, *Nat. Neurosci.* **2004**, *7*, 321 – 322; c) G. T. H. Van Kempen, H. T. vanderLeest, R. J. van den Berg, P. Eilers, R. H. S. Westerink, *Biophys. J.* **2011**, *100*, 968 – 977; d) L. J. Mellander, R. Trouillon, M. I. Svensson, A. G. Ewing, *Sci. Rep.* **2012**, *2*, 907.

[22] D. Choquet, A. Triller, *Nat. Rev. Neurosci.* **2003**, *4*, 251 – 265.

[23] a) T. Karashima, *Br. J. Pharmacol.* **1981**, *72*, 673 – 684; b) T. B. Bolton, W. A. Large, *Quart. J. Exp. Physiol.* **1986**, *71*, 1 – 28.

Received: April 26, 2015
Published online: June 16, 2015

